Biomaterials 30 (2009) 4550–4557

Contents lists available at ScienceDirect

Biomaterials

journal homepage: www.elsevier.com/locate/biomaterials

Synthesis of highly porous crosslinked elastin hydrogels and their interaction with fibroblasts *in vitro*

Nasim Annabi [a], Suzanne M. Mithieux [b], Elizabeth A. Boughton [c], Andrew J. Ruys [c], Anthony S. Weiss [b], Fariba Dehghani [a,*]

[a] School of Chemical and Biomolecular Engineering, University of Sydney, Sydney, NSW 2006, Australia
[b] School of Molecular and Microbial Biosciences, University of Sydney, Sydney, NSW 2006, Australia
[c] School of Aerospace, Mechanical and Mechatronic Engineering, University of Sydney, Sydney, NSW 2006, Australia

ARTICLE INFO

Article history:
Received 3 April 2009
Accepted 10 May 2009
Available online 4 June 2009

Keywords:
Elastin
Hydrogel
Crosslinking
Hexamethylene diisocyanate
High pressure CO_2
Fibroblast

ABSTRACT

In this study the feasibility of using high pressure CO_2 to produce porous α-elastin hydrogels was investigated. α-Elastin was chemically crosslinked with hexamethylene diisocyanate that can react with various functional groups in elastin such as lysine, cysteine, and histidine. High pressure CO_2 substantially affected the characteristics of the fabricated hydrogels. The pore size of the hydrogels was enhanced 20-fold when the pressure was increased from 1 bar to 60 bar. The swelling ratio of the samples fabricated by high pressure CO_2 was also higher than the gels produced under atmospheric pressure. The compression modulus of α-elastin hydrogels was increased as the applied strain magnitude was modified from 40% to 80%. The compression modulus of hydrogels produced under high pressure CO_2 was 3-fold lower than the gels formed at atmospheric conditions due to the increased porosity of the gels produced by high pressure CO_2. The fabrication of large pores within the 3D structures of these hydrogels substantially promoted cellular penetration and growth throughout the matrices. The highly porous α-elastin hydrogel structures fabricated in this study have potential for applications in tissue engineering.

1. Introduction

Porous, three-dimensional (3D) scaffolds have been used extensively as biomaterials in tissue engineering since they may act as an analogue of the extracellular matrix and provide a physical support structure for cellular growth [1]. Scaffold mechanical properties and microstructure including porosity, mean pore size, interconnectivity, and surface area may influence, sometimes significantly, cell adhesion and infiltration [2–6]. Many natural hydrogels containing collagen, hyaluronic acid (HA), fibrin, alginate, agarose, dextran, chitosan, and elastin-like polypeptides (ELPs) are attractive materials that have been used as scaffolds due to their similarities with the extracellular matrix, excellent biological performance, and inherent cellular interaction capabilities [7,8]. Elastin is an insoluble extracellular matrix protein that provides tissues with the properties of elasticity and resilience [9]. Due to the presence of crosslinks in elastin, the protein is highly insoluble and therefore difficult to process into new biomaterials. Consequently, soluble forms of elastin including tropoelastin [10], α-elastin [11,12], and elastin-like polypeptides (ELPs) [13] are frequently used to form crosslinked hydrogels.

Various crosslinking methods including chemical [10–24], enzymatic [14,25], physical [26–28], and γ-irradiation [29–31] have been used to fabricate elastin-based hydrogels. The reactions may be carried out in an aqueous or organic phase depending on the type of crosslinker and desired properties of hydrogel. McMillan et al. [19] showed that crosslinking of an ELP in an organic solvent, where the ELP molecules exhibit no inverse phase transition, resulted in the formation of hydrogels that were more uniform and homogenous compared with those crosslinked in an aqueous solution. This process commonly comprises two steps: coacervation and crosslinking [19]. The dissimilarity observed between these hydrogels fabricated in aqueous and organic solutions presumably resulted from differences in interactions between the protein and the solvent during the crosslinking reaction [19]. In this study homogenous and non-porous hydrogels were obtained when the protein was chemically crosslinked in an organic solvent in the absence of coacervation [19]. In general, lack of cellular growth into

* Corresponding author. Tel.: +61 2 9351 4794; fax: +61 2 9351 2854.
E-mail address: fdehghani@usyd.edu.au (F. Dehghani).

0142-9612/$ – see front matter © 2009 Elsevier Ltd. All rights reserved.
doi:10.1016/j.biomaterials.2009.05.014

the 3D structures of ELP hydrogels due to the presence of small pores or porosity gradient is an issue associated with the current methods used for ELP hydrogel formation.

Dense gas carbon dioxide (CO_2) has been used widely as a gas foaming agent to induce porosity in the structure of amorphous or semi-crystalline hydrophobic polymers such as poly(lactic acid) (PLA), poly(lactic acid-*co*-glycolic acid) (PLGA), and polycaprolactone (PCL) [32–36]. A dense gas is a fluid at above or close to its critical temperature and pressure with the properties intermediate to those of gases and liquids. Dense gas CO_2 with a low critical temperature (T_c: 31 °C) is attractive for biomaterial processing because it is inert, non-toxic, and non-flammable [32,33].

Porous hydrogels have been fabricated using supercritical CO_2–water emulsion templated techniques [37–39] and also using dense gas CO_2 as a medium for crosslinking reactions [7,12,40,41]. The supercritical CO_2–water emulsion templated methodology has been successfully employed to produce highly porous crosslinked structures of different polymers such as dextran [38], chitosan [39], alginate [37], polyvinyl alcohol (PVA), and blended PVA/poly ethylene glycol (PEG) [39]. A 3D structure of highly interconnected and thin-walled porous dextran hydrogel with the average pore size less than 26 μm was formed using a surfactant to stabilise the CO_2–water emulsion [38]. Lee et al. synthesised a biodegradable and inexpensive poly(vinyl acetate)-based surfactant that can be used in this process to promote the product biocompatibility [39]. Further research may be required to enhance the pore sizes of these hydrogels for tissue engineering applications.

We have shown previously that highly porous α-elastin hydrogels can be formed by crosslinking α-elastin with glutaraldehyde (GA) in an aqueous solution using high pressure CO_2 [12]. These hydrogels were formed rapidly, in less than an hour, with pore structures resembling natural elastin [12]. Fibroblast cells proliferated in the 3D structures as a result of CO_2 induced channels within the structure of the α-elastin hydrogels [12]. The low mechanical properties of the hydrogels were attributed to the low number of lysine residues (less than 1%) in α-elastin that were available for crosslinking with GA.

The objective of this study was to fabricate α-elastin hydrogels with increased porosity and mechanical properties using hexamethylene diisocyanate (HMDI) as a crosslinking agent. Hexamethylene diisocyanate is a bifunctional molecule with lower cytotoxicity than GA [42]. In general, isocyanates may react with nucleophilic functional groups such as amines, alcohols, and protonated acids. Hexamethylene diisocyanate, in particular, reacts with the side chains of lysine, cysteine, and histidine, and to a lesser extent tyrosine, in water [21]. Therefore, HMDI may react with other amino acids available in the α-elastin structure to increase the crosslinking density and mechanical properties of fabricated hydrogels. Dimethyl sulfoxide (DMSO) was used as a solvent to fabricate HMDI crosslinked hydrogels due to the low solubility of HMDI in aqueous solution. Our research objective was to create an enhanced 3D pore network throughout α-elastin hydrogels, during the crosslinking process, by dissolving high pressure CO_2 into a DMSO solution, where the dissolved CO_2 would be released on depressurisation. The pore morphology, swelling ratio, and mechanical properties of the hydrogels fabricated in this CO_2 system were compared with those produced at atmospheric conditions. *In vitro* studies were also conducted to assess the cellular growth and proliferation in the 3D structures of fabricated hydrogels.

2. Materials and methods

2.1. Materials

α-Elastin extracted from bovine ligament was obtained from Elastin Products Co. (Missouri, USA). Dimethyl sulfoxide (DMSO) and hexamethylene diisocyanate (HMDI) were purchased from Sigma. Food grade carbon dioxide (99.99% purity) was supplied by BOC. GM3348 fibroblast cell line was obtained from the Coriell Cell Repository. Cells were maintained in Dulbecco's Modified Eagle's Medium (DMEM) supplemented with 10% v/v fetal bovine serum (FBS), penicillin and streptomycin. All tissue culture reagents were obtained from Sigma.

2.2. Hydrogel formation

2.2.1. Hydrogel fabrication at atmospheric pressure

In each experiment 100 mg/ml α-elastin in DMSO was mixed with HMDI and the solution was immediately pipetted into a glass Lab-Tek chamber slide. The sample was allowed to react for 18 h at room temperature under nitrogen. The crosslinked hydrogels were then swelled in MilliQ water and gently agitated on a shaker for 2 h to remove residual DMSO. The media were exchanged with fresh MilliQ water every 15 min with shaking. The hydrogels were then stored in PBS.

A preliminary set of experiments were conducted to determine the required amount of HMDI for the hydrogel fabrication. α-Elastin solutions at 100 mg/ml were mixed with various concentrations of HMDI ranging between 0.25% (v/v) and 10% (v/v). The solutions were then pipetted into Lab-Tek chamber slides and placed in a chamber connected to a nitrogen line for 18 h at room temperature (25 °C). The results demonstrated that hydrogels were formed at HMDI concentrations above 1% (v/v). At low concentrations of HMDI, dissolved α-elastin was partially crosslinked, while at high concentrations of HMDI (10%) the hydrogel was very rigid and non-elastic. Consequently, in this study, 2% (v/v) and 5% (v/v) HMDI were used to produce hydrogels.

2.2.2. Dense gas hydrogel formation

The experimental apparatus used to fabricate α-elastin hydrogels using dense gas CO_2 involved a high-pressure vessel coupled with a CO_2 source and a high-pressure pump. This apparatus has been previously described [12]. An α-elastin solution containing HMDI was injected into a custom-made Teflon mould placed inside the high-pressure vessel. After the vessel was sealed and approached thermal equilibrium at 25 °C, the system was pressurised with CO_2 to 60 bar, isolated and maintained at these conditions for a set period of time. The system was then depressurised and samples were collected. Then the crosslinked structures were swelled in MilliQ water and gently agitated on a shaker for 2 h to remove the residue of DMSO. The hydrogels were stored in PBS for further analysis.

2.3. Scanning electron microscopy (SEM)

The SEM images of samples were obtained using a Philips XL30 scanning electron microscope (15 kV) to determine the pore characteristics of the fabricated hydrogels and to examine cellular infiltration and adhesion. Lyophilised α-elastin hydrogels were mounted on aluminium stubs using conductive carbon paint, then gold coated prior to SEM analysis.

Cell-seeded hydrogels were fixed with 2% (v/v) GA in 0.1 M Na-cacodylate buffer with 0.1 M sucrose for 1 h at 37 °C. Samples underwent post-fixation with 1% osmium in 0.1 M Na-cacodylate for 1 h and were then dehydrated in ethanol solutions at 70%, 80%, 90% and 3 times 100% for 10 min each. For drying, the samples were immersed for 3 min in 100% hexamethyldisilazane (HMDS) then transferred to a desiccator for 25 min to avoid water contamination. Finally they were mounted on stubs and sputter coated with 10 nm gold.

2.4. Mechanical characterisation: compressive properties

Uniaxial compression tests were performed in an unconfined state using a Bose ELF3400 mechanical tester with a 50 N load cell. The testing procedure was done in accordance with previously documented hydrogel mechanical testing reports [43–45]. Prior to mechanical testing, the hydrogels produced at high pressure CO_2 and atmospheric condition were swelled for 2 h in PBS. The thickness (3 ± 0.1 mm) and diameter (12.5 ± 0.7 mm) of each sample were measured using a digital calliper prior to mechanical testing. The compressive properties of the samples were tested in the hydrated state, in PBS, at room temperature. Compression (mm) and load (N) were recorded using Wintest software at a cross speed of 30 μm/s and different strain levels ranging from 40% to 80%. At each strain level, the samples were cyclically preconditioned for 7 cycles to minimize artefact interference. The hydrogels were subsequently subjected to another loading and unloading cycle (8th cycle) where compression (mm) and load (N) were collected. At each strain level, the compressive modulus for the 8th cycle was obtained as the tangent slope of the stress–strain curve. In addition, at each strain level, the energy loss based on the 8th compression cycle was computed. Three specimens were tested for each sample type (sample produced at high pressure CO_2 or atmospheric pressure) at each strain level.

2.5. Swelling property

The swelling behaviours of the HMDI crosslinked hydrogels produced at high pressure CO_2 and atmospheric conditions were evaluated at room temperature (25 °C) in three different solvent environments: MilliQ water, phosphate-buffered

saline (PBS), and DMSO. All hydrogels were lyophilised prior to use and were weighed dry. The samples were then swelled in 10 ml of solvent (MilliQ water, PBS or DMSO) for 24 h. For each solvent, at least three samples were placed in the media overnight. The excess liquid was then removed from the swelled samples and the swelling ratio was calculated based on the ratio of the increase in mass to that of the dry sample.

2.6. In vitro cell culture

The ability of human skin fibroblast cells (GM3348) to grow into the 3D hydrogel structure was assessed. Following crosslinking, hydrogels were transferred into a 48-well plate and washed twice with ethanol to sterilise the materials. The hydrogels were then washed at least twice with culture media to remove any residual ethanol and equilibrated in culture media (DMEM, 10% FBS, pen-strep) at 37 °C overnight. The cells were then seeded onto the hydrogels at 1.6×10^5 cells/well and compared with unseeded hydrogel in an adjacent well. Cells were cultured in a CO_2 incubator for 3 days at 37 °C, after which the hydrogels were fixed to assess cell proliferation and infiltration using light microscopy and SEM analysis.

2.7. Light microscopy analysis on histological samples

The growth of the cells in fabricated hydrogels was confirmed using light microscopy analysis after fixing, sectioning, and staining cross-sections of cell-seeded scaffolds. The hydrogels containing cells were fixed by soaking in 10% formalin overnight. The scaffolds were then immersed in 70% ethanol. The samples were processed on an automated tissue processor on a 6 h cycle to paraffin through a graded series of ethanol, and xylene. They were embedded in paraffin wax and 5 μm sections were taken and collected onto glass slides and dried. The slides were then deparaffinised, rehydrated, stained using a standard haematoxylin and eosin staining procedure, dehydrated, cleared in xylene, and mounted in DPX. The cross-sections were examined using a light microscope (Olympus DP50) connected to the camera.

3. Results and discussion

In this study the feasibility of using high pressure CO_2 to produce HMDI crosslinked α-elastin hydrogels with increased mechanical properties and pore sizes was assessed. The effects of reaction time and crosslinker concentration on the characteristics of the hydrogel produced at high pressure CO_2 were investigated. Preliminary experiments demonstrated that when 2% (v/v) HMDI was used, the hydrogels were not formed at reaction times below 2 h. A partially crosslinked film of α-elastin was observed in the mould when the system was depressurised after 1 h. However, when the crosslinker concentration was increased to 5% (v/v), a hydrogel with desirable pore size and elasticity was obtained within 1 h. As the reaction time was further increased from 1 to 2 h, the 5% (v/v) HMDI crosslinked hydrogel became rigid and less elastic.

3.1. Pore structure of the α-elastin hydrogel

The structures of hydrogels including porosity, pore sizes, and interconnectivity have a substantial influence on penetration, adhesion, and growth of the cells within the 3D structures. The macrostructures of 2% (v/v) HMDI crosslinked α-elastin hydrogels produced at high pressure CO_2 and atmospheric conditions in lyophilised and hydrated states are shown in Fig. 1. Rigid α-elastin hydrogels were formed at both high pressure CO_2 and atmospheric conditions as shown in Fig. 1. The hydrogels were easily handled and kept their macrostructures after swelling. This was due to the high degree of crosslinking within the structures of HMDI crosslinked hydrogels. As shown in Fig. 1, increased porosity in the hydrogels fabricated at high pressure was clearly evident.

In this study, SEM analysis was used to characterise the pore morphology of fabricated α-elastin hydrogels. As shown in Fig. 2c–f, the hydrogels fabricated at 60 bar CO_2 pressure were highly porous. Comparison of SEM images of α-elastin hydrogels produced under high pressure CO_2 and atmospheric conditions indicated that high pressure CO_2 increased the pore size of the fabricated hydrogels as shown in Fig. 2. Equivalent circle diameter (ECD) of the pores was calculated using Image J software. The average pore size of hydrogels fabricated by using 2% (v/v) HMDI increased from 3.9 ± 0.8 μm to 79.8 ± 54.8 μm when pressure was increased from 1 bar to 60 bar. In hydrogels fabricated by the dense gas CO_2, 52.6% of the pores were above 80 μm in diameter which makes these hydrogels suitable for cellular growth through the 3D structures. The presence of large channels in the cross-sections of samples fabricated at high pressure CO_2 (Fig. 2d) could facilitate cellular penetration and proliferation into the 3D structures. These large channels were not present in hydrogels fabricated at atmospheric conditions as shown in Fig. 2b. The generation of large channels is a unique feature of dense gas CO_2 that facilitated the penetration and growth of fibroblast cells in 3D structures of GA crosslinked α-elastin hydrogels reported in our previous study [12].

The formation of large pores in the 3D structures of HMDI crosslinked hydrogels produced at high pressure CO_2 may be due to the high solubility of CO_2 in DMSO at operating temperature (25 °C) and pressure (60 bar). Phase behaviour studies on binary mixtures of CO_2 and DMSO indicated that solubility of CO_2 in DMSO is a function of temperature and pressure [46]. Kordikowski et al. reported that increasing the temperature decreased the CO_2 solubility in DMSO. The solubility of CO_2 in DMSO was also enhanced by increasing the pressure at constant temperature [46]. The molar fractions of CO_2 increased from 0.1 to 0.9 when pressure raised from 10 bar to 60 bar at 25 °C [46]. The extent of miscibility is reflected in the volume expansions of the liquid phase; no further expansion takes place with the occurrence of liquid–liquid immiscibility. The volume expansions for the binary mixture of CO_2 and DMSO increased from 10% to 820% at 25 °C when pressure was increased from 10 bar to 60 bar [46]. However, using a higher temperature (30 °C) the volume expansions of the mixture increased from 6.5% to 180% when pressure was enhanced from 10 bar to 60 bar [46]. Consequently, in this study the operating conditions of 25 °C and 60 bar were used to achieve higher solubility of CO_2 in DMSO. α-Elastin solution in DMSO could be expanded by CO_2 at 60 bar and 25 °C as the crosslinking

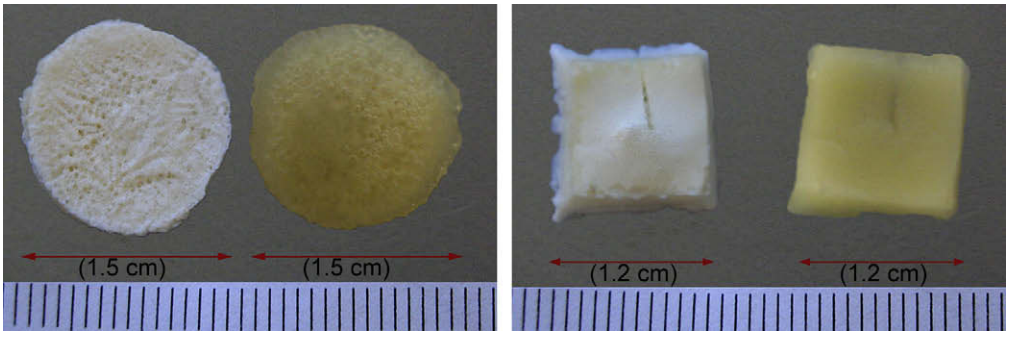

Fig. 1. HMDI crosslinked α-elastin hydrogel produced at 60 bar CO_2 (a), and atmospheric conditions (b) before and after hydration in water at 25 °C.

reaction and gelation took place. The presence of the crosslinker in the α-elastin solution is likely to limit the expansion of α-elastin solution by CO_2.

Using 5% (v/v) HMDI, the number of the large pores on the top and also in the cross-section of the sample was reduced as compared to the 2% (v/v) HMDI crosslinked hydrogels (Fig. 2 e and f). However, using a higher concentration of HMDI (5% (v/v)), the hydrogels were more rigid than 2% (v/v) HMDI crosslinked hydrogels. Increasing the crosslinker concentration resulted in an increase in the degree of crosslinking through the hydrogel matrices, which limited the ability of the α-elastin solution to expand in CO_2 and led to the formation of smaller pores.

3.2. Mechanical characterisation: compressive properties

The compressive mechanical properties of HMDI crosslinked samples produced at high pressure CO_2 and atmospheric conditions are shown in Fig. 3. The compression modulus of both samples, produced at high pressure and atmospheric conditions, increased as the applied strain magnitude was increased. The compression modulus of the sample produced at atmospheric conditions ranged from 11.25 ± 0.4 kPa to 18.8 ± 3.4 kPa at 40% and 80% strain, respectively (Fig. 3c). The stress-strain curve became nonlinear at strain levels above 40% as shown in Fig. 3b. This indicated that plastic deformation occurred in the hydrogels produced at atmospheric conditions at strains greater than 40%. However, for the samples fabricated at high pressure CO_2, the stress–strain curve was still linear at 60% strain (Fig. 3a). Therefore, the samples produced at high pressure CO_2 were expected to be more elastic than hydrogels produced at atmospheric conditions. The compression modulus of the HMDI crosslinked hydrogel produced by high pressure CO_2 ranged from 3.99 ± 0.5 kPa to 8.62 ± 1.7 kPa at 40% and 80% strain, respectively (Fig. 3c). The compression modulus of the hydrogels produced at high pressure CO_2 was generally lower than the samples produced at atmospheric conditions. This means that the samples produced at atmospheric pressure were stiffer than those produced using high pressure CO_2. This was expected due to the increased porosity of the samples fabricated at high pressure CO_2.

The compression properties of the fabricated materials were comparable to those reported in the literature for a number of biomaterials. Srokowski et al. found that the compression modulus of a non-porous ELP gel was between 6.26 kPa and 215 kPa over a strain range of 20–80% [43]. However, for a porous foam-like ELP

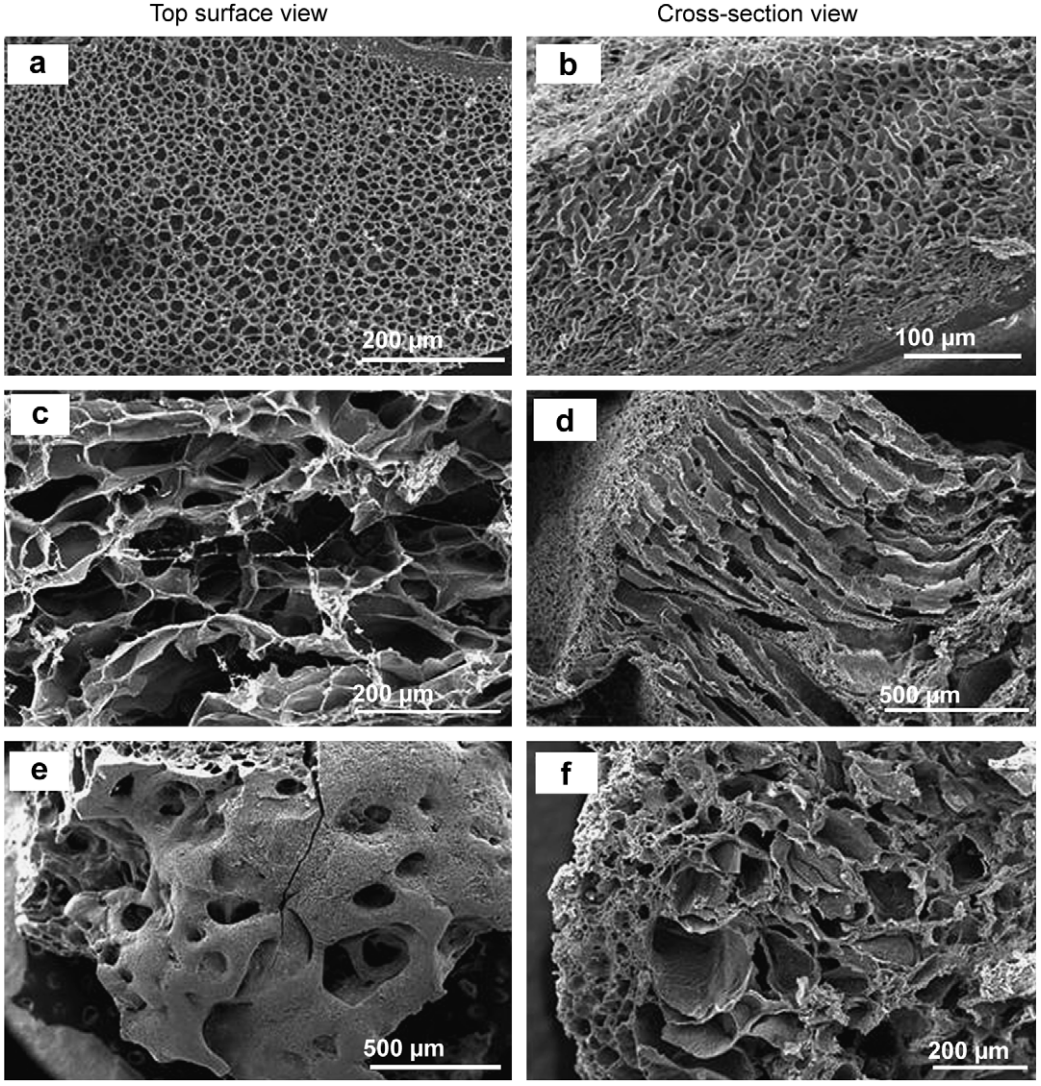

Fig. 2. SEM images of α-elastin hydrogels fabricated at atmospheric pressure using 2% HMDI (a, b), 60 bar CO_2 pressure using 2% HMDI (c, d), 60 bar CO_2 pressure using 5% HMDI (e, f).

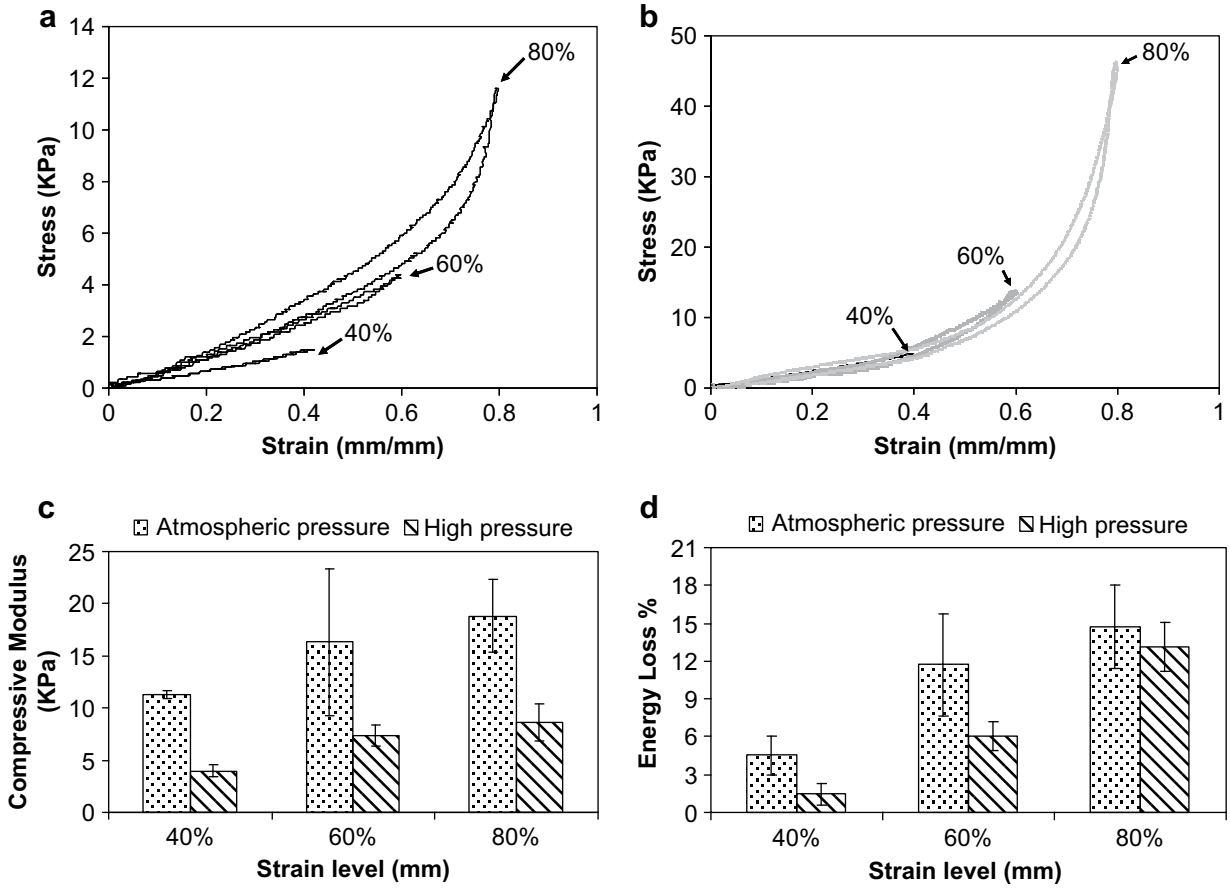

Fig. 3. Unconfined compressive behaviour of HMDI crosslinked hydrogel. Cyclic stress–strain data for the sample produced at high pressure CO_2 (a), and atmospheric condition (b). Compressive modulus (c) and energy loss (d) at each strain level for both hydrogels produced at high pressure CO_2 and atmospheric conditions.

the compression modulus was reported between 4.48 kPa and 146.50 kPa [43]. The compression strength of a flexible polyurethane foam increased from 2.4 kPa to 11.7 kPa for strain levels between 20% and 60% as reported by Lutter et al. [47]. Thomas et al. fabricated a copolymer gel of polyvinyl alcohol (PVA)/polyvinyl pyrrolidine (PVP) for endoscopic replacement of the nucleus pulposus of a lumbar intervertebral disk [48]. The compression modulus of fabricated PVA/PVP was reported between 4 kPa and 5.5 kPa for 15% and 25% in strain level [48]. The compression modulus of a poly(ethylene glycol) diacrylate (PEGDA) used for lamina propria regeneration ranged between ~30 kPa and 100 kPa depending on the PEGDA concentration [49]. The compression modulus of porous natural–synthetic polymer composites, produced by impregnation monomers such as butylmethacrylate (BMA) into porous alginate using emulsion templating and supercritical CO_2, was also reported between 9.8 ± 3.7 kPa and 39.9 ± 4.2 kPa by Partap et al. [50]. The mean compressive modulus of the nucleus pulposus of the lumbar intervertebral disc was reported to be 5.4 kPa [51] which is in the range of the compressive modulus of fabricated α-elastin hydrogel using high pressure CO_2. As the intervertebral disc consists of approximately 1.7% elastin [52], the HMDI crosslinked hydrogels at high pressure CO_2 offer unique promise for an orthopaedic application.

High resilience of elastin provides the ability to deform reversibly without loss of energy [53]. Energy loss is proportional to hysteresis. Using 60% strain level, the energy loss for the hydrogels fabricated at high pressure CO_2 was $6.03 \pm 1.14\%$. However, for the gels produced at atmospheric conditions the energy loss was $11.72 \pm 4.02\%$, demonstrating greater hysteresis for the samples produced at atmospheric pressure. As shown in Fig. 3d, the energy loss of both hydrogels fabricated at high pressure CO_2 and atmospheric conditions increased with increasing strain levels. The energy loss for samples produced at high pressure CO_2 increased from $1.43 \pm 0.86\%$ to $13.16 \pm 1.93\%$, when the strain level increased from 40% to 80% as shown in Fig. 3d. For the hydrogels produced at atmospheric pressure, it increased from $4.51 \pm 1.54\%$ to $14.67 \pm 3.31\%$ when the strain level increased from 40% to 80%.

The energy loss of the fabricated α-elastin hydrogel was either lower or comparable with those reported for fabricated ELPs using various crosslinkers. Veith et al. found that the energy loss for a genipin crosslinked elastin-based recombinant polypeptide was $9.7 \pm 6.2\%$ [24]. However, using pyrroloquinoline quinone (PQQ) as a crosslinking agent, energy loss increased to $20.4 \pm 1.6\%$ indicating greater hysteresis in PQQ crosslinked sheets [24]. Srokowski et al. also reported a relatively constant energy loss of $51.3 \pm 10.1\%$ at different strain levels for an ELP [43]. The energy loss of aorta elastin purified from porcine tissue was reported to be $23 \pm 2\%$ by Bellingham et al. and for two different engineered ELPs $20 \pm 7\%$ and $23 \pm 10\%$ [20].

3.3. Swelling properties

The swelling behaviour of the fabricated hydrogels is shown in Fig. 4. Generally, the swelling ratio of the samples exposed to high pressure CO_2 was higher than the hydrogels fabricated at atmospheric condition as indicated in Fig. 4. Both hydrogels produced at high pressure CO_2 and atmospheric pressure swelled more in DMSO than in water and PBS. Hydrogels produced at 60 bar CO_2

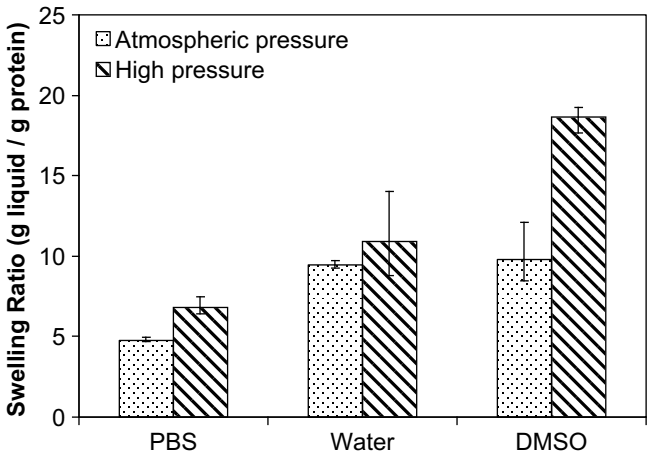

Fig. 4. Swelling behaviour of hydrogels produced at high pressure CO_2 and atmospheric conditions in PBS, water, and DMSO.

Table 1
Swelling ratio and compressive modulus of hydrogels fabricated at high pressure CO_2 and atmospheric conditions.

Crosslinked hydrogel	Swelling ratio (g liquid/g protein)	Compressive modulus (kPa)
Atmospheric pressure	9.82 ± 1.97	11.25 ± 0.4[a] 18.8 ± 3.4[b]
High pressure	18.65 ± 0.88	3.99 ± 0.5[a] 8.62 ± 1.7[b]

[a] Applied strain magnitude: 40%.
[b] Applied strain magnitude: 80%.

pressure absorbed 6.81 ± 0.46, 10.9 ± 2.46, and 18.65 ± 0.88 g liquid/g protein when they were hydrated in PBS, water, and DMSO, respectively. However, the gels formed at atmospheric pressure absorbed 4.79 ± 0.15, 9.45 ± 0.25, and 9.82 ± 1.97 g liquid/g protein when they were swelled in PBS, water, and DMSO, respectively. The exact mechanism of an increase in the swelling ratio of HMDI crosslinked hydrogels in DMSO is unknown [43]. DMSO can destabilize the secondary structure of proteins and peptides by interacting with the polypeptide backbone [43]. Lillie and Gosline reported that higher swelling in DMSO may be attributed to an increase in the molecular mobility of the elastin network through plasticisation [54]. In the DMSO system the α-elastin hydrogel may be plasticised by DMSO, resulting in an increase in segment length between crosslinks. The higher swelling ratio of the sample produced at high pressure CO_2 was due to the presence of larger pores through their structures compared to the hydrogel formed at atmospheric pressure.

The swelling ratio of HMDI crosslinked α-elastin hydrogels produced at high pressure CO_2 was either considerably greater or comparable with other crosslinked ELP hydrogels using diisocyanate crosslinker [21,43]. The swelling behaviour of α-elastin hydrogels produced at high pressure CO_2 was comparable with a lysine diisocyanate (LDI) crosslinked ELPs with the swelling capacity of approximately 6 g liquid/g protein in both PBS and water [43]. However, the swelling ratio of gels produced at high pressure CO_2 was 10-fold higher than an HMDI crosslinked ELPs reported by Nowatzki et al. (0.37 g H_2O/g protein at 4 °C) [21]. This may be due to the increased porosity within the structures of fabricated hydrogels or lower degree of crosslinking.

The swelling ratio of HMDI crosslinked α-elastin using 60 bar CO_2 pressure was lower than the GA crosslinked α-elastin hydrogel fabricated at 60 bar CO_2, which was 33.2 ± 0.8 g H_2O/g protein as reported in our previous study [12]. This may due to the higher degree of crosslinking through the structures of HMDI crosslinked α-elastin hydrogel as the swelling ratio of hydrogels is correlated to the degree of crosslinking. Generally, the hydrogels with a high degree of crosslinking exhibit low swelling ratio.

The swelling behaviour of the HMDI crosslinked hydrogel was correlated with the compressive modulus. In general, the samples with greater swelling have lower compressive moduli as indicated in Table 1. This phenomenon has also been reported by Srokowski et al., where a higher compressive modulus corresponded to lower level of swelling for LDI crosslinked hydrogels [43]. Vieth et al. also found that the elastic modulus of genipin crosslinked ELPs was irreversibly correlated with the swelling ratio [24].

3.4. *In vitro fibroblast cell proliferation using elastin hydrogels*

Cellular growth and proliferation in α-elastin hydrogels were examined by light microscopy and SEM analysis to demonstrate the feasibility of using the processed material for soft tissue engineering applications. The light microscopy images of adherent fibroblast cells cultured on hydrogel produced at 60 bar CO_2 are shown in Fig. 5. Haematoxylin and eosin were used for staining, as a result the cells appear as dark grey and the α-elastin scaffolds as light grey. As shown in Fig. 5b and c fibroblast cells were able to grow into the 3D structures of α-elastin due to the presence of large pores induced by high pressure CO_2. However, cells were only able to form a monolayer on the surface of the hydrogel fabricated at atmospheric conditions as indicated in Fig. 5a, due to the presence of small pores on the surface. The SEM images in Fig. 6 corroborated the cell proliferation into the 3D structure of hydrogel fabricated at high pressure CO_2. As shown in Fig. 6, cells were able to colonise at the top surface (Fig. 6b and c) and also into the 3D structure (Fig. 6d–f) of α-elastin hydrogels produced under high pressure CO_2 due to the presence of large pores within the materials.

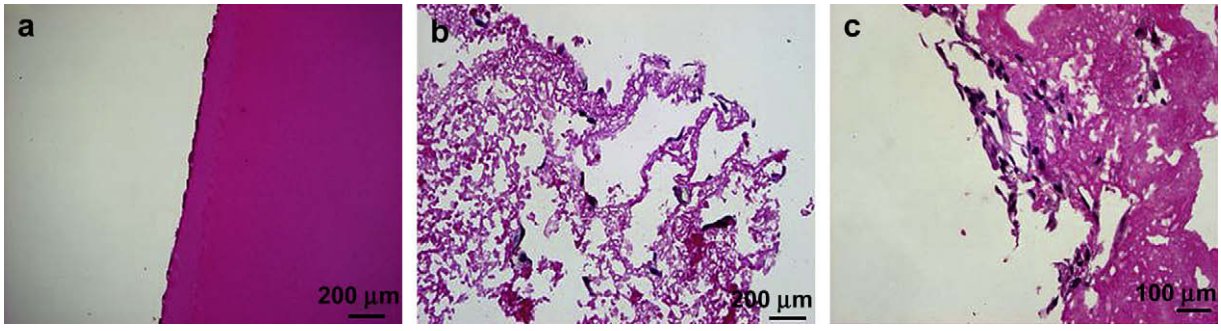

Fig. 5. Images of fibroblast cells cultured on hydrogel produced at atmospheric pressure (a) and high pressure CO_2 (b and c).

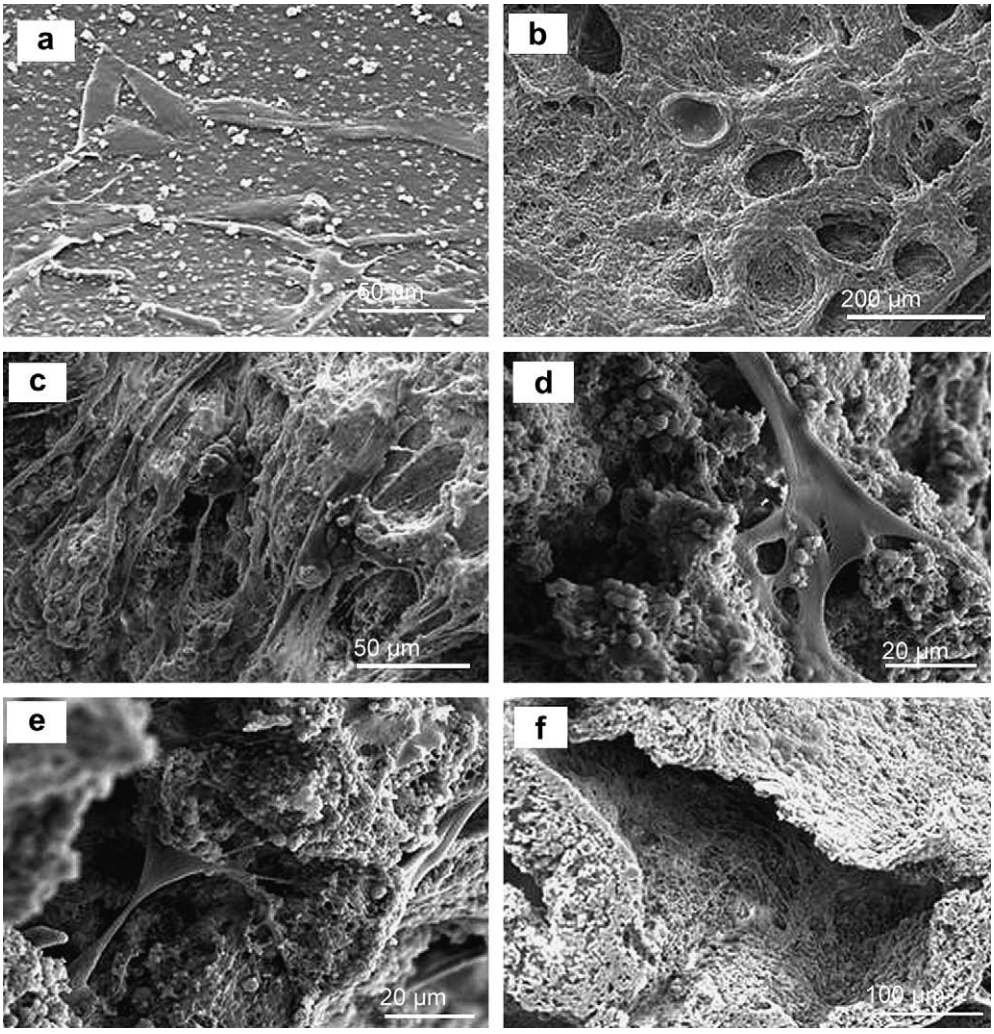

Fig. 6. SEM images of fibroblast cells attached to α-elastin hydrogel fabricated at atmospheric conditions (a), and high pressure CO_2 (b–f). Top surfaces (a–c), internal surfaces of hydrogel obtained by cross sectioning the sample (d–f).

4. Conclusions

This study demonstrated the feasibility of fabricating elastin hydrogels with enhanced mechanical properties and pore sizes using dense gas CO_2 and HMDI crosslinker. High pressure CO_2 significantly increased the pore sizes of fabricated hydrogels due to the high solubility and diffusion of CO_2 in DMSO. Hydrogels fabricated using dense gas CO_2 were more elastic compared with those fabricated at atmospheric pressure. The compressive modulus of the sample produced at high pressure CO_2 was lower than the gel fabricated at atmospheric conditions due to the presence of larger pores within the structures of crosslinked material produced under high pressure CO_2. The fabrication of these large pores within the 3D structures substantially promoted fibroblast infiltration and growth throughout the matrices. The fabricated α-elastin hydrogels display promising characteristics that may be suitable for soft tissue repair and orthopaedic applications such as spinal nucleus replacement.

Acknowledgements

The authors acknowledge financial support from Sydnovate, the Australian Research Council (AW), and Merck Pty Ltd.

Appendix

Figures with essential colour discrimination. Fig. 5 in this article may be difficult to interpret in black and white. The full colour images can be found in the on-line version, at doi:10.1016/j.biomaterials.2009.05.014.

References

[1] Liu C, Xia Z, Czernuszka JT. Design and development of three-dimensional scaffolds for tissue engineering. Chem Eng Res Des 2007;85(A7):1051–64.
[2] Harley BA, Leung JH, Silva ECCM, Gibson LJ. Mechanical characterization of collagen–glycosaminoglycan scaffolds. Acta Biomater 2007;3(4):463–74.
[3] O'Brien FJ, Harley BA, Yannas IV, Gibson LJ. The effect of pore size on cell adhesion in collagen–GAG scaffolds. Biomaterials 2005;26(4):433–41.
[4] Zeltinger J, Sherwood JK, Graham DA, Mueller R, Griffith LG. Effect of pore size and void fraction on cellular adhesion, proliferation, and matrix deposition. Tissue Eng 2001;7(5):557–72.
[5] Nehrer S, Breinan HA, Ramappa A, Young G, Shortkroff S, Louie LK, et al. Matrix collagen type and pore size influence behavior of seeded canine chondrocytes. Biomaterials 1997;18(11):769–76.
[6] Wake MC, Patrick Jr CW, Mikos AG. Pore morphology effects on the fibrovascular tissue growth in porous polymer substrates. Cell Transplant 1994;3(4):339–43.
[7] Temtem M, Casimiro T, Mano JF, Aguiar-Ricardo A. Green synthesis of a temperature sensitive hydrogel. Green Chem 2007;9(1):75–9.

[8] Malafaya PB, Silva GA, Reis RL. Natural-origin polymers as carriers and scaffolds for biomolecules and cell delivery in tissue engineering applications. Adv Drug Deliv Rev 2007;59(4–5):207–33.
[9] Mithieux SM, Weiss AS. Elastin. Adv Protein Chem 2005;70:437–61.
[10] Mithieux SM, Rasko JEJ, Weiss AS. Synthetic elastin hydrogels derived from massive elastic assemblies of self-organized human protein monomers. Biomaterials 2004;25(20):4921–7.
[11] Leach JB, Wolinsky JB, Stone PJ, Wong JY. Crosslinked alpha-elastin biomaterials: towards a processable elastin mimetic scaffold. Acta Biomater 2005;1(2):155–64.
[12] Annabi N, Mithieux SM, Weiss AS, Dehghani F. The fabrication of elastin-based hydrogels using high pressure CO_2. Biomaterials 2009;30(1):1–7.
[13] Lim DW, Nettles DL, Setton LA, Chilkoti A. In situ cross-linking of elastin-like polypeptide block copolymers for tissue repair. Biomacromolecules 2008;9(1):222–30.
[14] Mithieux SM. Synthetic elastin: construction and properties of cross-linked human tropoelastin. Ph.D. dissertation. Sydney, NSW: University of Sydney; 2003.
[15] Welsh ER, Tirrell DA. Engineering the extracellular matrix: a novel approach to polymeric biomaterials. I. Control of the physical properties of artificial protein matrices designed to support adhesion of vascular endothelial cells. Biomacromolecules 2000;1(1):23–30.
[16] Martino M, Tamburro AM. Chemical synthesis of cross-linked poly(KGGVG), an elastin-like biopolymer. Biopolymers 2001;59(1):29–37.
[17] McMillan RA, Caran KL, Apkarian RP, Conticello VP. High-resolution topographic imaging of environmentally responsive, elastin-mimetic hydrogels. Macromolecules 1999;32(26):9067–70.
[18] Di Zio K, Tirrell DA. Mechanical properties of artificial protein matrixes engineered for control of cell and tissue behavior. Macromolecules 2003;36(5):1553–8.
[19] McMillan RA, Conticello VP. Synthesis and characterization of elastin–mimetic protein gels derived from a well-defined polypeptide precursor. Macromolecules 2000;33(13):4809–21.
[20] Bellingham CM, Lillie MA, Gosline JM, Wright GM, Starcher BC, Bailey AJ, et al. Recombinant human elastin polypeptides self-assemble into biomaterials with elastin-like properties. Biopolymers 2003;70(4):445–55.
[21] Nowatzki PJ, Tirrell DA. Physical properties of artificial extracellular matrix protein films prepared by isocyanate crosslinking. Biomaterials 2003; 25(7–8):1261–7.
[22] Trabbic-Carlson K, Setton LA, Chilkoti A. Swelling and mechanical behaviors of chemically cross-linked hydrogels of elastin-like polypeptides. Biomacromolecules 2003;4(3):572–80.
[23] Lim DW, Nettles DL, Setton LA, Chilkoti A. Rapid cross-linking of elastin-like polypeptides with (hydroxymethyl)phosphines in aqueous solution. Biomacromolecules 2007;8(5):1463–70.
[24] Vieth S, Bellingham CM, Keeley FW, Hodge SM, Rousseau D. Microstructural and tensile properties of elastin-based polypeptides crosslinked with genipin and pyrroloquinoline quinone. Biopolymers 2007;85(3):199–206.
[25] McHale Melissa K, Setton Lori A, Chilkoti A. Synthesis and in vitro evaluation of enzymatically cross-linked elastin-like polypeptide gels for cartilaginous tissue repair. Tissue Eng 2005;11(11–12):1768–79.
[26] Mithieux Suzanne M, Tu Y, Korkmaz E, Braet F, Weiss Anthony S. In situ polymerization of tropoelastin in the absence of chemical cross-linking. Biomaterials 2009;30(4):431–5.
[27] Nagapudi K, Brinkman WT, Thomas BS, Park JO, Srinivasarao M, Wright E, et al. Viscoelastic and mechanical behavior of recombinant protein elastomers. Biomaterials 2005;26(23):4695–706.
[28] Nagapudi K, Brinkman WT, Leisen J, Thomas BS, Wright ER, Haller C, et al. Protein-based thermoplastic elastomers. Macromolecules 2005;38(2):345–54.
[29] Lee J, Macosko CW, Urry DW. Phase transition and elasticity of protein-based hydrogels. J Biomater Sci Polym Ed 2001;12(2):229–42.
[30] Lee J, Macosko CW, Urry DW. Mechanical properties of cross-linked synthetic elastomeric polypentapeptides. Macromolecules 2001;34(17):5968–74.
[31] Lee J, Macosko CW, Urry DW. Swelling behavior of γ-irradiation cross-linked elastomeric polypentapeptide-based hydrogels. Macromolecules 2001; 34(12):4114–23.
[32] Quirk RA, France RM, Shakesheff KM, Howdle SM. Supercritical fluid technologies and tissue engineering scaffolds. Curr Opin Solid State Mater Sci 2005;8(3–4):313–21.
[33] Tai H, Popov VK, Shakesheff KM, Howdle SM. Putting the fizz into chemistry: applications of supercritical carbon dioxide in tissue engineering, drug delivery and synthesis of novel block copolymers. Biochem Soc Trans 2007;35(3):516–21.
[34] Barry JJA, Silva MMCG, Popov VK, Shakesheff KM, Howdle SM. Supercritical carbon dioxide: putting the fizz into biomaterials. Philos Trans R Soc London Ser A 2006;364(1838):249–61.
[35] Cansell F, Aymonier C, Loppinet-Serani A. Review on materials science and supercritical fluids. Curr Opin Solid State Mater Sci 2003;7(4–5): 331–40.
[36] Barry JJA, Gidda HS, Scotchford CA, Howdle SM. Porous methacrylate scaffolds: supercritical fluid fabrication and in vitro chondrocyte responses. Biomaterials 2004;25(17):3559–68.
[37] Partap S, Rehman I, Jones JR, Darr JA. Supercritical carbon dioxide in water emulsion-templated synthesis of porous calcium alginate hydrogels. Adv Mater 2006;18(4):501–4.
[38] Palocci C, Barbetta A, La Grotta A, Dentini M. Porous biomaterials obtained using supercritical CO_2–water emulsions. Langmuir 2007;23(15):8243–51.
[39] Lee J-Y, Tan B, Cooper AI. CO_2-in-water emulsion-templated poly(vinyl alcohol) hydrogels using poly(vinyl acetate)-based surfactants. Macromolecules 2007;40(6):1955–61.
[40] Cooper AI, Holmes AB. Synthesis of molded monolithic porous polymers using supercritical carbon dioxide as the porogenic solvent. Adv Mater 1999;11(15): 1270–4.
[41] Cooper AI, Wood CD, Holmes AB. Synthesis of well-defined macroporous polymer monoliths by sol–gel polymerization in supercritical CO_2. Ind Eng Chem Res 2000;39(12):4741–4.
[42] Van Luyn MJA, Van Wachem PB, Damink LO, Dijkstra PJ, Feijen J, Nieuwenhuis P. Relations between in vitro cytotoxicity and crosslinked dermal sheep collagens. J Biomed Mater Res 1992;26(8):1091–110.
[43] Srokowski EM, Woodhouse KA. Development and characterisation of novel cross-linked bio-elastomeric materials. J Biomater Sci Polym Ed 2008;19(6): 785–99.
[44] Stammen JA, Williams S, Ku DN, Guldberg RE. Mechanical properties of a novel PVA hydrogel in shear and unconfined compression. Biomaterials 2001;22(8):799–806.
[45] Joshi A, Fussell G, Thomas J, Hsuan A, Lowman A, Karduna A, et al. Functional compressive mechanics of a PVA/PVP nucleus pulposus replacement. Biomaterials 2006;27(2):176–84.
[46] Kordikowski A, Schenk AP, Van Nielen RM, Peters CJ. Volume expansions and vapor–liquid equilibria of binary mixtures of a variety of polar solvents and certain near-critical solvents. J Supercrit Fluids 1995;8(3):205–16.
[47] Lutter HD, Hinz W, Decker W, Leppkes R, Reich E, Peters R, et al., inventors. Block polyoxyethylene–polyoxypropylene polyols for the production of flexible polyurethane foams with low compression hardness. US Patent No. 5,059,633; 1991.
[48] Thomas J, Gomes K, Lowman A, Marcolongo M. The effect of dehydration history on PVA/PVP hydrogels for nucleus pulposus replacement. J Biomed Mater Res B Appl Biomater 2004;69(2):135–40.
[49] Liao H, Munoz-Pinto D, Qu X, Hou Y, Grunlan Melissa A, Hahn Mariah S. Influence of hydrogel mechanical properties and mesh size on vocal fold fibroblast extracellular matrix production and phenotype. Acta Biomater 2008;4(5):1161–71.
[50] Partap S, Hebb AK, Rehman I, Darr JA. Formation of porous natural–synthetic polymer composites using emulsion templating and supercritical fluid assisted impregnation. Polym Bull 2007;58(5–6):849–60.
[51] Umehara S, Tadano S, Abumi K, Katagiri K, Kaneda K, Ukai T. Effects of degeneration on the elastic modulus distribution in the lumbar intervertebral disc. Spine 1996;21(7):811–9. discussion 820.
[52] Mikawa Y, Hamagami H, Shikata J, Yamamuro T. Elastin in the human intervertebral disk: a histological and biochemical study comparing it with elastin in the human yellow ligament. Arch Orthop Trauma Surg 1986;105(6): 343–9.
[53] Gosline J, Lillie M, Carrington E, Guerette P, Ortlepp C, Savage K. Elastic proteins: biological roles and mechanical properties. Philos Trans R Soc Lond B Biol Sci 2002;357(1418):121–32.
[54] Lillie MA, Gosline JM. Swelling and viscoelastic properties of osmotically stressed elastin. Biopolymers 1996;39(5):641–52.